Pergamon

SCIENCE DIRECT®

Tetrahedron 59 (2003) 3709–3718

TETRAHEDRON

Synthesis and properties of novel 5-(cyclohepta-2′,4′,6′-trienylidene)pyrimidine-2(1*H*),4(3*H*),6(5*H*)-triones: methodology for synthesizing cyclohepta[*b*]pyrimido[5,4-*d*]furan-8(7*H*),10(9*H*)-dionylium tetrafluoroborates

Shin-ichi Naya and Makoto Nitta*

Department of Chemistry, School of Science and Engineering, Waseda University, Shinjuku-ku, Tokyo 169-8555, Japan

Received 19 February 2003; revised 1 April 2003; accepted 3 April 2003

Abstract—Novel condensation reaction of tropone with *N*-substituted and *N*,*N*′-disubstitued barbituric acids in Ac_2O afforded 5-(cyclohepta-2′,4′,6′-trienylidene)pyrimidine-2(1*H*),4(3*H*),6(5*H*)-trione derivatives (**8a**–**f**) in moderate to good yields. The ^{13}C NMR spectral study of **8a**–**f** revealed that the contribution of zwitterionic resonance structures is less important as compared with that of 8,8-dicyanoheptafulvene. The rotational barriers ($\Delta G^{\ddagger}$) around the exocyclic double bond of mono-substituted derivatives **8a**–**c** were obtained to be 14.51–15.03 kcal mol^{-1} by the variable temperature ^1H NMR measurements. The electrochemical properties of **8a**–**f** were also studied by CV measurement. Upon treatment with DDQ, **8a**–**c** underwent oxidative cyclization to give two products, 7 and 9-substituted cyclohepta[*b*]pyrimido[5,4-*d*]furan-8(7*H*),10(9*H*)-dionylium tetrafluoroborates (**11a**–**c**·BF_4^- and **12a**–**c**·BF_4^-) in various ratios, while that of disubstituted derivatives **8d**–**f** afforded 7,9-disubstituted cyclohepta[*b*]pyrimido[5,4-*d*]furan-8(7*H*),10(9*H*)-dionylium tetrafluoroborate (**11d**–**f**·BF_4^-) in good yields. Similarly, preparation of known 5-(1′-oxocycloheptatrien-2′-yl)-pyrimidine-2(1*H*),4(3*H*),6(5*H*)-trione derivatives (**14a**–**d**) and novel derivatives **14e**,**f** was carried out. Treatment of **14a**–**c** with aq. HBF_4/Ac_2O afforded two kinds of novel products **11a**–**c**·BF_4^- and **12a**,**c**·BF_4^- in various ratios, respectively, while that of **14d**–**f** afforded **11d**–**f**. The product ratios of **11a**–**c**·BF_4^- and **12a**–**c**·BF_4^- observed in two kinds of cyclization reactions were rationalized on the basis of MO calculations of model compounds **20a** and **21a**. The spectroscopic and electrochemical properties of **11a**–**f**·BF_4^- and **12a**–**c**·BF_4^- were studied, and structural characterization of **11c**·BF_4^- based on the X-ray crystal analysis and MO calculation was also performed.

1. Introduction

Heptafulvenes have intrigued chemists for several decades, especially in the context of the concept of aromaticity.[1–3] The properties and chemical behavior of substituted heptafulvenes are usually rationalized in terms of the differing contribution of the zwitterionic resonance structures. The relative contribution of such canonicical structures depends on the electronegativity of the substituents at the 8-position, which modulates the aromaticity of the ring. Thus, 8,8-dicyanoheptafulvene (**1a**) (Fig. 1) and its derivatives have been synthesized by the reaction of tropone (**6**) with active-methylene compounds, such as malononitrile,[4] and their properties and X-ray structure analysis have been studied.[5] The seven-membered ring of **1a** is nearly planar,[5] while that of **1b** is puckered.[6] Thus, the rotational barrier around the exocyclic double bond of heptafulvenes **2a**–**c** and their derivatives has been investigated to evaluate the steric effect between the C2 or C7-substituents and C8 substituents as well as the contribution

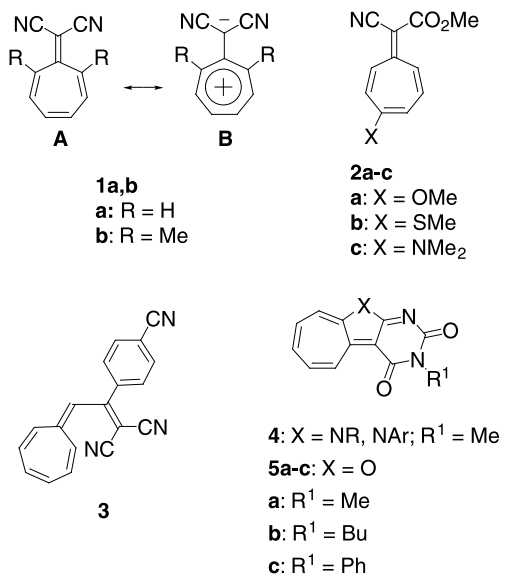

Figure 1.

Keywords: 5-(cyclohepta-2′,4′,6′-trienylidene)pyrimidine-2(1*H*),4(3*H*),6(5*H*)-trione; cyclohepta[*b*]pyrimido[5,4-*d*]furan-8(7*H*),10(9*H*)-dionylium tetrafluoroborate; uracil-annulated heteroazulene; redox potential.

* Corresponding author. Tel.: +81-3-5286-3236; fax: +81-3-3208-2735; e-mail: nitta@waseda.jp

0040–4020/03/$ - see front matter
doi:10.1016/S0040-4020(03)00543-X

of the zwitterionic structure.[7] The chemistry of the extended cyclic cross-conjugated compounds derived by insertion of more complex conjugated π-systems instead of the exo-double bond of heptafulvene has also been studied relative to the molecular design of organic dyes, highly polarized compounds, and electron acceptors or electron donors.[8] Recently, the synthesis and photochemical properties of compound **3**, which is a more conjugated π-system of **1**, have been studied to demonstrate that compound **3** possesses a remarkable property of multimode-switching arising from the ring-closure and ring-opening process: a very fast photoreversible switch and a thermal switch.[9] Thus, the heptafulvenes having variety of conjugated functional groups seem to be interesting from the viewpoint of molecular function. We have previously studied convenient preparations of 6,9-disubstituted cyclohepta[*b*]-pyrimido[5,4-*d*]pyrrole-8(6*H*),10(9*H*)-diones (**4**) and 9-substituted cyclohepta[*b*]pyrimido[5,4-*d*]furan-8,10(9*H*)-dione (**5a–c**), which are structural isomers of 5-deaza-flavin[10–12] and 5-deaza-10-oxaflavin, respectively,[13] and their functions in oxidizing some alcohols to the corresponding carbonyl compounds.[14,15] In relation to these studies, we have previously studied the synthesis and properties of heteroazulene-substituted methyl cations[16–19] and tropylium ions.[20] The reduction potentials and pK_{R+} values of these cations clarified that heteroazulenes stabilize not only cations but also radical species. In this context, we have recently reported the synthesis and reactivity of 7,9-dimethylcyclohepta[*b*]pyrimido[5,4-*d*]furan-8(7*H*),10(9*H*)-dionylium tetrafluoroborate (**11d**·BF_4^-) (Scheme 3) as well as its photo-induced autorecycling oxidizing reactions toward some alcohols.[21] Thus, the uracil-annulated heteroazulenes are highly interesting from the viewpoint of oxidizing functions as in the case of 5-deazaflavin[10–12] and 5-deaza-10-oxaflavin,[13] and exploration of methodology for synthesizing various cyclohepta[*b*]pyrimido[5,4-*d*]furan-8(7*H*),10(9*H*)-dionylium tetrafluoroborate derivatives of **11d**·BF_4^- is required. We studied the synthesis and properties of a novel type of heptafulvenes, 5-(cyclohepta-2′,4′,6′-trienylidene)pyrimidine-2(1*H*),4(3*H*),6(5*H*)-trione (**8a–f**), which are converted to **11a–c**·BF_4^-, **12a–c**·BF_4^-, and **11d–f**·BF_4^-, respectively, upon treatment with DDQ. Similarly, synthesis of known 5-(1′-oxocycloheptatrien-2′-yl)-pyrimidine-2(1*H*),4(3*H*),6(5*H*)-trione derivatives (**14a–c**[15]) and novel derivative **14e,f** in addition to known **14d**[21] was performed, and they were treated with aq. HBF_4/Ac_2O to afford two kinds of products, **11a–f**·BF_4^- and **12a,c**·BF_4^-. The product ratios of **11a–c**·BF_4^- and **12a–c**·BF_4^- in both reactions of **8a–c** and **14a–c** are rationalized on the basis of MO calculations of the model compounds **20a** and **21a** as well. The spectroscopic and electrochemical properties of cations **11a–f** and **12a–c** are studied, and structural characterization of **11c**·BF_4^- based on the X-ray crystal analysis and MO calculation is also performed. We report herein the results in detail.

2. Results and discussion

2.1. Synthesis and properties of 8a–d

Condensation reactions of tropone (**6**) with barbituric acids **7a–f** in Ac_2O[22] under reflux afforded heptafulvenes **8a–f** as reddish needles in moderate to good yields (Scheme 1). The results are summarized in Table 1. The heptafulvenes **8a–f** were fully characterized on the basis of the ^1H and ^{13}C NMR, IR, UV–vis, and mass spectral data as well as elemental analyses.

In the ^{13}C NMR spectra, signals of carbon atoms (C-5 of the barbituric acid moiety) of **8a–f** appeared at δ_C 101.7–103.1. Since these signals are shifted to higher field as compared with those of **1a** and **2a–c** (**1a**: δ_C 70.1, **2a**: δ_C 87.5, **2b**: δ_C 89.0, and **2c**: δ_C 79.2),[7] the contributions of the zwitterionic canonical structure **B** (Scheme 1) seems to be less important than the canonical structure A, unlike in the cases of **1a** and **2a–c**. In the ^1H NMR spectra of **8a–c** at room temperature, the signals of H-2′ and H-7′ (Scheme 1) appear as two broad signals. These signals become equivalent at high-temperature (55°C), while they appear as two sharp doublets at low-temperature (−60°C). Thus,

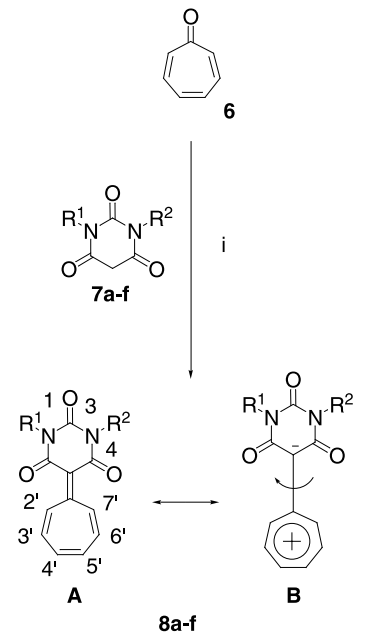

a: R^1 = Me, R^2 = H; **b**: R^1 = Bu, R^2 = H;
c: R^1 = Ph, R^2 = H; **d**: R^1 = R^2 = Me;
e: R^1 = R^2 = Et; **f**: R^1 = R^2 = Ph

Scheme 1. *Reagents and conditions*: i, Ac_2O, reflux, 0.5 h.

Table 1. Results for the preparation of heptafulvenes **8a–f** and their rotational barriers and redox potentials

Run	Barbituric acid **7a–f**	Condensation product (yield, %)	Rotational barrier[a] ($\Delta G^{\ddagger}$, kcal mol^{-1})	Redox potentials[b]	
				El_{ox}	El_{red}
1	**7a**	**8a** (77)	14.51	+1.08	−1.15
2	**7b**	**8b** (74)	14.70	+1.09	−1.19
3	**7c**	**8c** (62)	15.03	+1.11	−1.13
4	**7d**	**8d** (80)	–	+1.07	−1.23
5	**7e**	**8e** (83)	–	+1.07	−1.25
6	**7f**	**8f** (99)	–	+1.10	−1.18

[a] The rotation around the double bond between barbituric acid-moiety and cycloheptatrienylidene-moiety. Determined by the ^1H NMR signals of H-2′ and H-7′ of cycloheptatrienylidene-moiety.
[b] Peak potentials in V vs $Ag/AgNO_3$.

rotation around the exocyclic double bonds of **8a–c** clearly occurs slowly on the NMR time scale at room temperature. Through variable temperature ^{1}H NMR measurements of **8a–c**, the coalescence temperatures were determined to be 300, 308, and 315 K, respectively. In addition, the chemical shift differences between H-2′ and H-7′ of **8a–c** were 78 Hz, 105 Hz, and 108 Hz, respectively. Consequently, rotational barriers ($\Delta G^{\ddagger}$) around the exocyclic double bond for **8a–c** were determined to be 14.1–15.03 kcal mol^{-1} (Table 1). The values ($\Delta G^{\ddagger}$) of **8a–c** are in the order of **8a**<**8b**<**8c** and these are smaller than those of **2a–c** (16.32–23.30 kcal mol^{-1}); however, the contribution of the zwitterionic canonical structure **B** for **8a–c** is smaller than that of **2a–c**. This feature suggests that the steric hindrance between the H-2′, 7′ and two carbonyl-oxygens for **8a–c** is larger than that for **2a–c**. UV–vis spectra of **8a–f** in acetonitrile are shown in Figures 2 and 3. The spectra resemble each other and the longest wavelength absorption maxima of **8a–f** are similar (**8a**: 432 nm, **8b**: 432 nm, **8c**: 434 nm, **8d**: 431 nm, **8f**, 431 nm, and **8f**, 434 nm). In addition, the absorption maxima of **8a–f** appear at longer wavelength than that of **1** (384 nm).[23]

The redox property of heptafulvene **8a–f** was determined by cyclic voltammetry (CV) in acetonitrile. The oxidation and reduction waves of **8a–f** were irreversible under the conditions of CV measurements, and thus, the peak potentials are summarized in Table 1. The redox processes

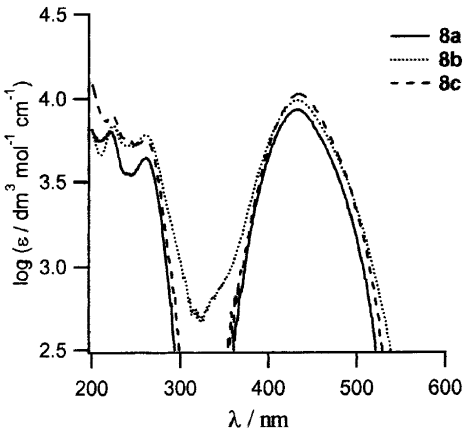

Figure 2. UV–vis spectra of **8a–c** in CH_3CN.

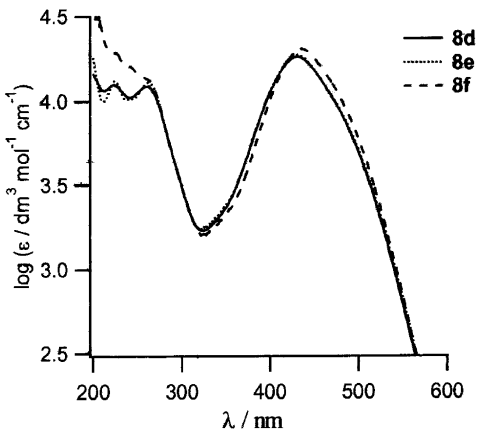

Figure 3. UV–vis spectra of **8d–f** in CH_3CN.

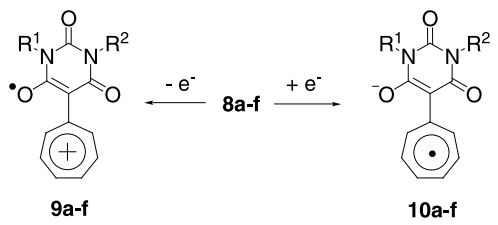

a: R^1 = Me, R^2 = H; **b**: R^1 = Bu, R^2 = H;
c: R^1 = Ph, R^2 = H; **d**: R^1 = R^2 = Me;
e: R^1 = R^2 = Et; **f**: R^1 = R^2 = Ph

Scheme 2.

of **8a–f** are depicted in Scheme 2. At the first oxidation potentials ($E1_{ox}$) of **8a–d**, radical cations **9a–f** would be generated, and radical anions **10a–f** seemed to be generated at the first reduction potentials ($E1_{red}$), respectively. After the first cycle of CV measurements of **8d–f**, other reduction waves were recorded at −0.58, −0.61, and −0.58 V, respectively. These waves are suggested to be the reduction waves of **11d–f**, which are generated by oxidative cyclization reactions of **9d–f** under CV measurement (vide infra).

2.2. Synthesis and properties of 11a–f·BF_4^- and 12a–c·BF_4^-

Reactions of **8a–c** and **8d–f** with DDQ in CH_2Cl_2 at room

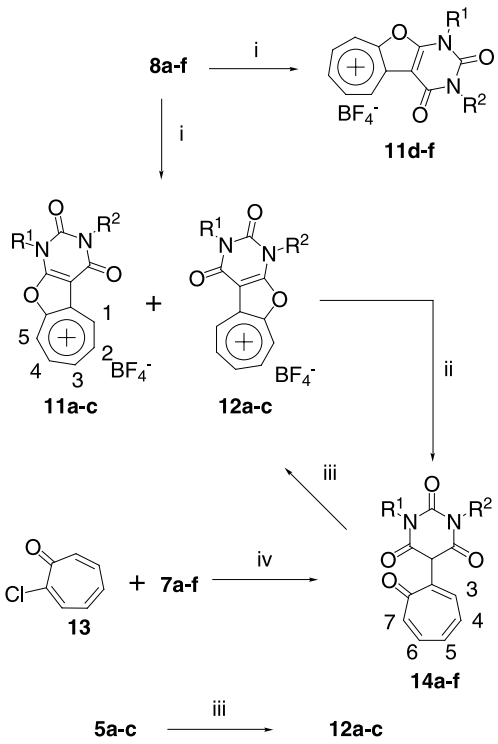

a: R^1 = Me, R^2 = H; **b**: R^1 = Bu, R^2 = H;
c: R^1 = Ph, R^2 = H; **d**: R^1 = R^2 = Me;
e: R^1 = R^2 = Et; **f**: R^1 = R^2 = Ph

Scheme 3. *Reagents and conditions*: i, (a) DDQ, CH_2Cl_2, rt, 1 h (b) 42% aq. HBF_4, Ac_2O, 0°C, 1 h; ii, aq. K_2CO_3, EtOH, 80°C, 12 h; iii, 42% aq. HBF_4, Ac_2O, 0°C, 1 h; iv, (a) Bu^{t}NH$_2$, rt, 16 h (b) 3% HCl.

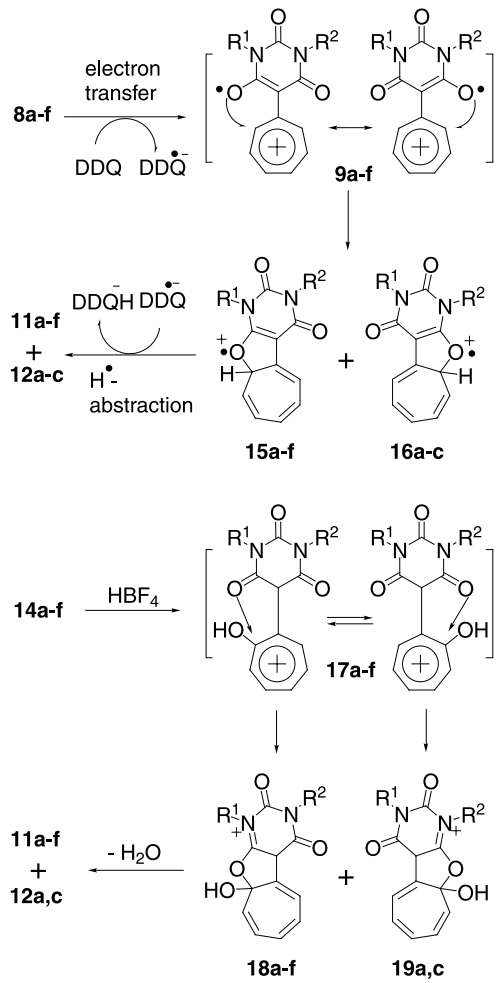

a: R^1 = Me, R^2 = H; **b**: R^1 = Bu, R^2 = H;
c: R^1 = Ph, R^2 = H; **d**: R^1 = R^2 = Me;
e: R^1 = R^2 = Et; **f**: R^1 = R^2 = Ph

Scheme 4.

temperature and subsequent anion exchange reaction using aq. HBF_4 in Ac_2O afforded mixtures of two products **11a**–**c**·BF_4^- and **12a**–**c**·BF_4^- and single products **11d**–**f**·BF_4^-, respectively (Scheme 3). Product ratios, which were determined by ^1H NMR as being preferential formation of **12a**–**c**·BF_4^-, and/or yields are summarized in Table 2. Mixtures of **11a**–**c**·BF_4^- and **12a**–**c**·BF_4^- could not be separated by recrystallization. On the other hand, we have reported previously that compounds **14a**–**d** can be obtained by the reactions of 2-chlorotropone **13** with **7a**–**d** (Scheme 3). Upon treatment with TFA, compounds **14a**–**c** were converted to **5a**–**c**.[15] Upon treatment with aq. HBF_4 in Ac_2O, however, **14d** was converted to **11d**·BF_4^- in 96% yield.[21] Thus, **14e**,**f** was prepared in a similar fashion, and compounds **14a**–**c** and **14e**,**f** were treated with aq. HBF_4 in Ac_2O to afford a mixture of **11a**·BF_4^- and **12a**·BF_4^-, **11b**·BF_4^-, a mixture of **11c**·BF_4^- and **12c**BF_4^-, and **11e**,**f**·BF_4^-, respectively (Scheme 3, Table 2). Contrary to the reactions of **8a**–**c** with DDQ, **14a**–**c** afforded compounds **11a**–**c**·BF_4^- preferentially. A mixture of two products **11a**·BF_4^- and **12a**·BF_4^- was not separated; however, pure samples of **11b**,**c**·BF_4^- were obtained by recrystallization. Furthermore, compounds **12a**–**c**·BF_4^- were obtained by protonation of **5a**–**c** with aq. HBF_4 in Ac_2O (Scheme 3, Table 2), and thus, assignment of the ^1H NMR spectrum of a mixture of **11a**·BF_4^- and **12a**·BF_4^- was performed. Thus, a mixture of **11a**·BF_4^- and **12a**·BF_4^- as well as compounds **11b**,**c**·BF_4^-, and **11e**,**f**·BF_4^-, and **12a**–**c**·BF_4^- were fully characterized on the basis of ^1H and ^{13}C NMR, IR, mass spectral data and elemental analyses. Mass spectra of these compounds exhibited the correct $M^+-BF_4^-$ ion peaks, which are indicative of the cationic structures of these compounds. The characteristic absorption bands for the counter ion of BF_4^- were observed at 1084–1085 cm^{-1} in the IR spectra of these compounds, respectively. In the ^1H NMR spectra, the proton signals on the seven-membered ring of **11a**–**c**·BF_4^- (**11a**: δ 8.67–9.44; **11b**: δ: 8.70–9.43; **11c**: δ 8.69–9.53), **12a**–**c**·BF_4^- (**12a**: δ 8.67–9.50: **12b**: δ 8.71–9.52; **12c**: δ 8.71–9.45), and **11e**,**f**·BF_4^- (**11e**: δ 8.70–9.52: **11f**: δ 8.73–9.58) appeared in lower field than those of **5a**–**c** (**5a**: δ 7.70–8.89; **5b**: δ 7.67–8.87; **5c**: δ 7.72–8.85).[15] These features also support the cationic nature of the compounds. UV–vis spectra of a mixture of **11a** and **12a**, **11b**,**c**, **12a**–**c**, and **11d**–**f** in acetonitrile are similar and the absorption maxima are summarized in Table 3. In the UV–vis spectra of **12a**–**c**, two absorption maxima were observed in the visible region, respectively. The longer wavelength absorption maxima are due to the generation of **5a**–**c** (**5a**: 439 nm; **5b**: 439 nm; **5c**: 445 nm), respectively, by a slight amount of deprotonation of **12a**–**c** under measurement conditions of UV–vis spectra and CV (vide infra). Upon addition of a drop of 42% aq. HBF_4 to the solutions of **12a**–**c**, respectively, the absorption of **5a**–**c** in the UV–vis spectra disappeared. In contrast, ^1H NMR measurements of **12a**–**c** did not exhibit proton signals of **5a**–**c**, respectively. In addition, upon treatment of the mixtures of **11a**–**c**·BF_4^- and **12a**–**c**·BF_4^- with aqueous K_2CO_3 solution at 80°C, ring-opening reaction occurs to afford **14a**–**c**, respectively (Scheme 3).

The selectivity of two types of cyclization reactions, oxidative cyclization of **8a**–**c** and acid-catalyzed cyclization

Table 2. Results for the preparation of cation **11a**–**f**·BF_4^- and **12a**–**c**·BF_4^-

Run	Oxidative cyclization of **8a**–**f**		Acidic dehydration of **14a**–**f**		Protonation of **5a**–**c**
	Product (yield, %)	Ratio of **11**/**12**	Product (yield, %)	Ratio of **11**/**12**	Product (yield, %)
1	**11a** (43), **12a** (47)	1:1.1	**11a** (62), **12a** (38)	1:0.6	**12a** (88)
2	**11b** (27), **12b** (67)	1:2.5	**11b** (80)	1:0.0	**12b** (97)
3	**11c** (23), **12c** (77)	1:3.3	**11c** (58), **12c** (6)	1:0.1	**12c** (99)
4	**11d** (86)	-	**11d** (96)	-	-
5	**11e** (100)	-	**11e** (100)	-	-
6	**11f** (99)	–	**11f** (100)	–	–

Table 3. UV–vis spectral data (in acetonitrile) of cations **11a–f** and **12a–c** (salts **11a–f**·BF_4^- and **12a–c**·BF_4^- were used for the measurements)

Compound	λ_{max} (nm) (log ε, $dm^3\ mol^{-1}\ cm^{-1}$)
11a[a]	395 (4.38), 269 (4.42), 223 (4.41)
11b	399 (4.67), 268 (4.41), 225 (4.42)
11c	398 (4.50), 264 (4.43), 257 (4.45), 222 (4.51)
11d[b]	397 (4.47), 267 (4.45), 224 (4.41)
11e	399 (4.49), 267 (4.43), 224 (4.41)
11f	396 (4.49), 262 (4.48), 224 (4.51)
12a	391 (4.44), 267 (4.45), 222 (4.35)
12b	392 (4.36), 267 (4.47), 222 (4.38)
12c	390 (4.44), 267 (4.40), 222 (4.46)

[a] A mixture of **11a**·BF_4^- and **12a**·BF_4^- was used for the measurement.
[b] Ref. 21.

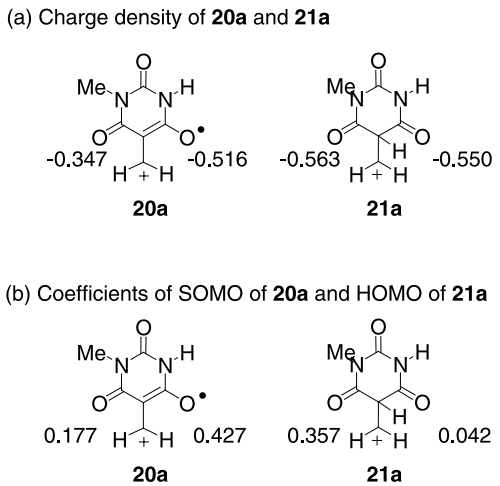

Figure 4.

of **14a–c**, affording **11a–c** and **12a–c** is explained as follows. According to the redox properties of **8a–f** under CV measurement (vide supra), we propose the former reaction pathway as outlined in Scheme 4. The radical cations **9a–f**, which are generated by oxidation of **8a–f** with DDQ, undergo cyclization reactions to give two kinds of intermediates **15a–f** and **16a–c**. The hydrogen abstractions of radical cations **15a–f** and **16a–c** by DDQ-radical anion give cations **11a–f** and **12a–c**, respectively. Thus, the ratios of **11a–c/12a–c** seem to depend on the selectivity of the intramolecular O-radical addition to the tropylium moiety in **9a–c**. On the other hand, the latter acid-catalyzed cyclization reaction of **14a–f** would proceed as shown also in Scheme 4. By using 3,5,7-trideuterio-2-chlorotropone, we have clarified that the cyclization reaction of **14d** giving **11d**·BF_4^- proceeds via C-1 attack on the tropone nucleus.[21] The cations **17a–f**, which are generated by protonation of **14a–f** with HBF_4, undergo cyclization reaction to give **18a–f** and **19a–c**. The dehydration from cations **18a–f** and **19a–c** gives cations **11a–f** and **12a–c**, respectively. Thus, the ratio of **11a–c/12a–c** is considered to depend on the selectivity of the intramolecular addition of barbituric acid-oxygen to the hydroxytropylium moiety in **17a–c**. In order to investigate the reactivity of the intermediates **9a–c** and **17a–c**, compounds **20a** and **21a** are selected as model compounds of **9a** and **17a**, respectively (Fig. 4), and their MO calculations were carried out by the 6-31G* basis set of the MP2 levels.[24] At the carbonyl-oxygen, the charge density of **20a** and **21a** as well as the coefficients of SOMO of **20a** and those of HOMO of **21a** are depicted in Figure 4. Regarding the charge density and the coefficients of SOMO for radical cation **20a**, both values are larger for the oxygen atom of –CONH– than those of –CONMe–, suggesting that cyclization of the former moiety occurs preferentially to that of the latter moiety, whether cyclization occurs charge-controlled or frontier orbital-controlled. Thus, the intermediates **9a–c** are postulated to have a tendency similar to **20a**; the formation of **16a–c** would be preferable to that of **15a–c** to result in the formation of compounds **12a–c**·BF_4^-. On the contrary, regarding the charge density and the coefficients of HOMO for cation **21a**, both values are larger for the oxygen atom of the –CONMe– moiety than those of the –CONH– moiety. Consequently, **18a–c** would be generated mainly to result in the preferable formation of **11a–c**·BF_4^- as compared with **12a–c**·BF_4^- (formation of **12b**·BF_4^- is not observed). Thus, the selectivity of oxidative cyclization of unsymmetrical heptafulvene **8a–c** and acid-catalyzed cyclization of **14a–c** seems to be rationalized.

The reduction property of cations **11a–c**, **11e**,**f**, and **12a–c** was determined by cyclic voltammetry (CV) in acetonitrile. The reduction waves of **11a–c**, **11e**,**f**, and **12a–c** were irreversible under the conditions of CV measurements, and thus, the peak potentials are summarized in Table 4, along with that of compound **11d**.[21] Since a mixture of **11a**·BF_4^- and **12a**·BF_4^- was not isolated, a mixture of **11a**·BF_4^- and **12a**·BF_4^- is used for the measurement of **11a**. The irreversible nature would be due to the formation of a tropyl radical and its dimerization. This reduction behavior seems to be a typical property of tropylium ions.[25] The $E1_{red}$ of cations **11a–f** and **12a–c** are similar to each other. In the CV measurement of **12a–c**, the reduction waves of **5a–c**, which derives from deprotonation of **12a–c**, were also observed. This feature is similar to that observed in the measurement of UV–vis spectra of **12a–c** (vide supra).

A single crystal of **11c**·BF_4^- was obtained by recrystallization from CH_3CN/Et_2O. Thus, X-ray structure analysis was carried out, and the ORTEP drawing of **11c**·BF_4^- is shown in Figure 5. The selected bond lengths are summarized in Table 5 (The numbering is shown in Figure 6). The bond lengths of C1–C2, C3–C4, and C5–C5a are shorter than those of C2–C3, C4–C5, C5a–C10b, and C10b–C1. This fact indicates the existence of bond alternation in the seven-membered ring as shown in canonical structures **11c-B** and **11c-C**. In addition, since the bond length of C5a–O6 is longer than that of O6–C6a, the contribution of **11c-D**

Table 4. Reduction potentials (peak potential in V vs $Ag/AgNO_3$) of cations **11a–f** and **12a–c** (salts **11a–f**·BF_4^- and **12a–c**·BF_4 were used for the measurements)

Compound	$E1_{red}$	Compound	$E1_{red}$
11a[a]	−0.58	**12a**	−0.56
11b	−0.59	**12b**	−0.57
11c	−0.57	**12c**	−0.55
11d[b]	−0.58		
11e	−0.61		
11f	−0.58		

[a] A mixture of **11a**·BF_4^- and **12a**·BF_4^- was used for the measurement.
[b] Ref. 21.

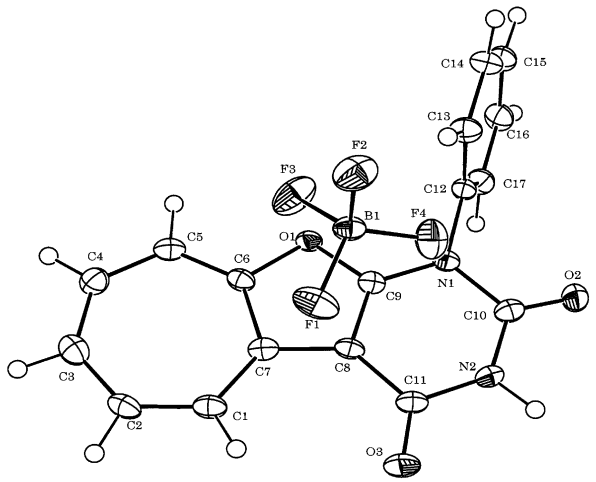

Figure 5. An ORTEP drawing of **11c** with thermal ellipsoid plot (50% probability).

oxidative cyclization of **8a–c** and acid-catalyzed cyclization of **14a–c** giving **11a–c**·BF_4^- and **12a–c**·BF_4^- was rationalized based on MO calculations of model compounds **20a** and **21a**. The structural characteristics of **11c**·BF_4^- were clarified for the first time by X-ray crystal analysis and MO calculations. Further studies concerning exploration of the functions of 5-(cyclohepta-2′,4′,6′-trienylidene)pyrimidine-2(1*H*),4(3*H*),6(5*H*)-trione derivatives and uracil-annulated heteroazulenylium ions are underway.

4. Experimental

4.1. General

IR spectra were recorded on a HORIBA FT-710 spectrometer. Mass spectra and high-resolution mass spectra were run on JMS-AUTOMASS 150 and JMS-SX102A spectrometers. The ^1H and ^{13}C NMR spectra were recorded on a JNM-lambda 500 and an AVANCE 600 spectrometers, and the chemical shifts are given relative to internal $SiMe_4$ standard: *J*-values are given in Hz. Mps are recorded on a Yamato MP-21 apparatus and are uncorrected. Compound **7d** is commercially available, and desired compounds **7a**,[26a] **7b**,**c**,[26b] **7e**,**f**,[26c] **14a–c**,[15] and **14d**[21] were prepared as described in the literature.

Table 5. Bond lengths of **11c**·BF_4 obtained by X-ray structure analysis and MO calculation

Cation	Method	Bond length[a]											
		C1–C2	C2–C3	C3–C4	C4–C5	C5–C5a	C5a–C10b	C10b–C1	C5a–O6	O6–C6a	C6a–N7	C6a–c10a	C10a–C10b
11c	X-Ray	1.38	1.40	1.38	1.39	1.36	1.43	1.40	1.38	1.34	1.34	1.37	1.42
11c	MP2/6-3lG*	1.38	1.41	1.39	1.41	1.37	1.43	1.41	1.38	1.35	1.33	1.38	1.41

[a] The numbering is shown in Figure 6.

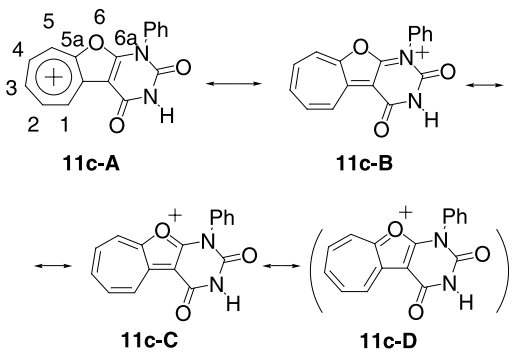

Figure 6.

seems to be less important. MO calculation of **11c** was carried out by the 6-31G* basis set of the MP2 levels[23] and the selected bond lengths are also summarized in Table 5. Concerning the seven-membered ring of **11c**, the bond lengths of C1–C2, C3–C4, and C5–C5a are shorter than those of C2–C3, C4–C5, C5a–C10b, and C10b–C1. The bond length alternation obtained by MO calculation for **11c** is very similar to that obtained by X-ray analysis.

3. Conclusion

The synthesis and properties of a novel type of heptafulvenes **8a–f** were investigated. The rotational barriers around the exocyclic double bond of **8a–c** were determined by variable temperature ^1H NMR measurements. Moreover, two types of synthetic methodology of **11a–f**·BF_4^- and **12a–c**·BF_4^- were established, and their spectroscopic and electrochemical properties were studied. The selectivity of

4.2. General synthetic procedure for 5-(cyclohepta-2′,4′,6′-trienylidene)pyrimidine-2(1*H*),4(3*H*),6(5*H*)-trione derivatives (8a–f)

A solution of **6** (106 mg, 1 mmol) and **7a–f** (1 mmol) in Ac_2O (2 mL) was heated under reflux for 0.5 h. After the reaction completed, the mixture was concentrated in vacuo and the resulting residue was purified by column chromatography on SiO_2 using AcOEt as the eluent to give the products **8a–f**. The results are summarized in Table 1.

4.2.1. Compound 8a. Reddish needles; mp 226–228°C (from CH_2Cl_2/EtOH); ^1H NMR (500 MHz, $CDCl_3$) δ 3.34 (3H, s, CH_3), 7.32–7.36 (2H, m, H-3′, 6′), 7.43–7.50 (2H, m, H-4′, 5′), 7.65 (1H, br, s, NH), 9.31 (1H, br, s, H-2′ or 7′), 9.33 (1H, br, s, H-2′ or 7′); ^{13}C NMR (125.7 MHz, $CDCl_3$) δ 27.6, 101.7, 140.0, 140.2, 140.5, 150.0, 162.8, 164.4, 165.2; IR ($CHCl_3$) ν 3408, 1714, 1662, 1623, 1387 cm^{-1}; MS (rel. int) *m/z* 230 (M^+, 100%); HRMS calcd for $C_{12}H_{10}N_2O_3$: 231.0770 (M+H). Found: 231.0806 (M^+ +H). Anal. calcd for $C_{12}H_{10}N_2O_3$+1/5H_2O: C, 61.64; H, 4.48; N, 11.98. Found: C, 61.3; H, 4.3; N, 12.1.

4.2.2. Compound 8b. Reddish needles; mp 141–142°C from (EtOH); ^1H NMR (500 MHz, $CDCl_3$) δ 0.95 (3H, t, *J*=7.4 Hz, Bu-4), 1.39 (2H, tq, *J*=7.6, 7.4 Hz, Bu-3), 1.63 (2H, quint., *J*=7.6 Hz, Bu-2), 3.92 (2H, t, *J*=7.6 Hz, Bu-1),

7.36–7.40 (2H, m, H-3′, 6′), 7.47–7.54 (2H, m, H-4′, 5′), 8.31 (1H, br s, NH), 9.28 (1H, br s, H-2′ or 7′), 9.39 (1H, br s, H-2′ or 7′); ^{13}C NMR (125.7 MHz, $CDCl_3$) δ 13.7, 20.2, 30.3, 41.0, 102.2, 139.5, 139.9, 149.9, 162.9, 164.1, 164.8; IR ($CHCl_3$) ν 3403, 1713, 1664, 1622, 1393 cm^{-1}; MS (rel. int.) *m/z* 272 (M^+, 68), 255 (3), 215 (50), 57 (100%). Anal. calcd for $C_{15}H_{16}N_2O_3$: C, 66.16; H, 5.92; N, 10.29. Found: C, 66.0, H, 5.7; N, 10.1.

4.2.3. Compound 8c. Reddish needles; mp 243–246°C (from EtOH, decomp.); ^{1}H NMR (500 MHz, $CDCl_3$) δ 7.24–7.26 (4H, m, H-3′, 6′, *o*-Ph), 7.38–7.41 (2H, m, H-4′, 5′), 7.41 (1H, t, *J*=7.4 Hz, *p*-Ph), 7.48 (2H, dd, *J*=7.9, 7.4 Hz, *m*-Ph), 7.78 (1H, br s, NH), 9.40 (2H, br s, H-2′, 7′); ^{13}C NMR (125.7 MHz, $CDCl_3$) δ 101.2, 128.7, 128.8, 129.3, 135.0, 140.5, 140.7, 141.1, 149.5, 162.9, 164.5, 165.8; IR ($CHCl_3$) ν 3396, 1718, 1669, 1635, 1380 cm^{-1}; MS (rel. int.) *m/z* 292 (M^+, 100%); HRMS cacld for $C_{17}H_{12}N_2O_3$: 293.0926 (M+H). Found: 293.0948 (M^++H). Anal. calcd for $C_{17}H_{12}N_2O_3$+1/2H_2O: C, 67.77; H, 4.35; N, 9.30. Found: C, 67.4; H, 4.1; N, 8.9.

4.2.4. Compound 8d. Reddish needles; mp 207–208°C (from CH_2Cl_2/EtOH); ^{1}H NMR (500 MHz, $CDCl_3$) δ 3.38 (6H, s, CH_3), 7.31–7.33 (2H, m, H-4′, 5′), 7.40–7.44 (2H, m, H-3′, 6′), 9.20 (2H, d, *J*=11.6 Hz, H-2′, 7′); ^{13}C NMR (125.7 MHz, $CDCl_3$) δ 28.4, 102.7, 138.9, 139.3, 139.6, 151.5, 163.4, 164.5; IR ($CHCl_3$) ν 1707, 1640, 1387, 1244 cm^{-1}; MS (rel. int.) *m/z* 244 (M^+, 100%). Anal. cacld for $C_{13}H_{12}N_2O_3$: C, 63.93; H, 4.95; N, 11.47. Found: C, 63.9; H, 4.8; N, 11.2.

4.2.5. Compound 8e. Reddish needles; mp 141–142°C (from AcOEt); ^{1}H NMR (500 MHz, $CDCl_3$) δ 1.24 (6H, t, *J*=7.1 Hz, Et-2), 4.03 (4H, q, *J*=7.1 Hz, Et-1), 7.24–7.30 (2H, m, H-4′, 5′), 7.34–7.41 (2H, m, H-3′, 6′), 9.14 (2H, d, *J*=11.2 Hz, H-2′, 7′); ^{13}C NMR (125.7 MHz) δ 13.4, 36.8, 103.1, 138.4, 138.9, 139.2, 150.6, 162.9, 164.2; IR ($CHCl_3$) ν 1705, 1635, 1398, 1296 cm^{-1}; MS (ESI) *m/z* (M^++H). Anal. calcd for $C_{15}H_{16}N_2O_3$; C, 66.16; H, 5.92; N, 10.29. Found: C, 66.1; H, 6.0; N, 10.4.

4.2.6. Compound 8f. Reddish needles; mp 264–265°C (from AcOEt); ^{1}H NMR (500 MHz, $CDCl_3$) δ 7.32 (4H, d, *J*=11.4 Hz, *o*-Ph), 7.38–7.42 (4H, m, *p*-Ph, H-4′, 5′), 7.45–7.50 (6H, m, *m*-Ph, H-3′, 6′), 9.38 (2H, d, *J*=11.4 Hz, H-2′, 7′); ^{13}C NMR (125.7 MHz) δ 101.9, 128.5, 128.8, 129.2, 135.6, 139.9, 140.1, 140.8, 150.7, 163.6, 165.7; IR ($CHCl_3$) ν 1718, 1653, 1375, 1258 cm^{-1}; MS (ESI) *m/z* 369 (M^++H); HRMS calcd for $C_{23}H_{16}N_2O_3$: 369.1239 (M+H). Found: 369.1217 (M^++H). Anal. calcd for $C_{23}H_{16}N_2O_3$+1/5H_2O: C, 74.26; H, 4.44; N, 7.53. Found: C, 74.5; H, 4.2; N, 7.5.

4.3. General oxidative cyclization of 8a–f with DDQ

To a stirred solution of **8a–f** (0.20 mmol) in CH_2C1_2 (10 mL) was added DDQ (70 mg, 0.3 mmol) and the mixture was stirred at rt for 1 h until the reaction completed. After evaporation of the CH_2C1_2, the residue was dissolved in a mixture of Ac_2O (2 mL) and 42% aq. HBF_4 (0.4 mL) at 0°C and the mixture was stirred for 1 h. To the mixture was added Et_2O (40 mL) and the precipitates were collected by filtration and washed with ether to give mixtures of **11a–c**·BF_4^- and **12a–c**·BF_4^- and **11d–f**·BF_4^-. The results are summarized in Table 2. The cation **11d**·BF_4^- was identical with the authentic specimen.[21]

4.4. General synthetic procedure for 5-(1′-oxocyclo-heptatrien-2′-yl)-pyrimidine-2(1*H*),4(3*H*),6(5*H*)-trione derivatives (14a–c and 14e,f)

A solution of 2-chlorotropone (**13**) (422 g, 3 mmol), 2(1*H*),4(3*H*),6(5*H*)-pyrimidinetrione derivatives (**7a–c** and **7e**,**f**) (3 mmol), and Bu^tNH_2 (548 g, 7.5 mmol) in MeOH (30 mL) was stirred at rt for 24 h. After evaporation of the MeOH and Bu^tNH_2, the residue was filtered and washed with Et_2O. The crystals were dissolved in 3% HC1 and extracted with CH_2C1_2. The extract was dried over Na_2SO_4 and concentrated in vacuo to give **14a–c** and **14e**,**f** (**14a**: 716 mg, 97%, **14b**: 868 mg, 91%, **14c**: 924 mg, 100%, **14e**: 864 mg, 100%, **14f**: 1152 mg, 100%).

4.4.1. Compound 14a. Colorless powder; mp 202–204°C (from AcOEt, decomp.); ^{1}H NMR (400 MHz, CD_3OD) δ 3.25 (3H, s, CH_3), 7.11 (1H, d, *J*=12.0 Hz, H-7), 7.27–7.35 (2H, m), 7.44–7.50 (1H, m), 7.70–7.78 (1H, m); ^{13}C NMR (150.9 MHz, $CDC1_3$) δ 28.1, 56.9, 133.7, 135.6, 137.4, 140.4, 141.2, 148.1, 150.0, 165.6, 167.1, 185.1; IR ($CHC1_3$) ν 1722, 1691, 1574 cm^{-1}; MS (FAB) *m/z* 247 (M^++H). Anal. calcd for $C_{12}H_{10}N_2O_4$: C, 58.54; H, 4.09; N, 11.38. Found: C, 58.4; H, 3.9; N, 11.6.

4.4.2. Compound 14b. Colorless powder; mp 179–181°C (from AcOEt, decomp.); ^{1}H NMR (400 MHz, CD_3OD) δ 0.95 (3H, t, *J*=7.1 Hz, Bu-4), 1.37 (2H, sex, *J*=7.1 Hz, Bu-3), 1.59 (2H, quint, *J*=7.1 Hz, Bu-2), 3.85 (2H, t, *J*=7.1 Hz, Bu-1), 7.11 (1H, d, *J*=12.0 Hz, H-7), 7.26–7.36 (2H, m), 7.43–7.50 (1H, m), 7.69–7.77 (1H, m); ^{13}C NMR (150.9 MHz, $CDC1_3$) δ 13.6, 20.0, 29.8, 41.6, 57.0, 133.6, 135.5, 137.3, 140.4, 141.2, 148.2, 150.0, 166.0, 166.9, 185.1; IR ($CHC1_3$) ν 1724, 1688, 1574 cm^{-1}; MS (FAB) *m/z* 289 (M^++H). Anal. calcd for $C_{15}H_{16}N_2O_4$: C, 62.49; H, 5.59; N, 9.72. Found: C, 62.2; H, 5.7; N, 9.8.

4.4.3. Compound 14c. Colorless powder; mp 201–203°C (from AcOEt, decomp.); ^{1}H NMR (400 MHz, CD_3OD) δ 7.16 (1H, d, *J*=12.0 Hz, H-7), 7.24–7.33 (4H, m), 7.38–7.52 (4H, m), 7.72–7.79 (1H, m); ^{13}C NMR (150.9 MHz, CD_3OD) δ 97.2, 129.8, 129.9, 130.2, 135.7, 136.1, 137.2, 139.9, 141.5, 142.9, 150.1, 152.6, 169.1, 169.8, 187.3; IR ($CHC1_3$) ν 1721, 1704, 1572 cm^{-1}; MS (FAB) *m/z* 309 (M^++H); HRMS calcd for $C_{17}H_{12}N_2O_4$: 309.0875 (M+H). Found: 309.0870 (M^++H). Anal. calcd for $C_{17}H_{12}N_2O_4$+1/5H_2O: C, 65.47; H, 4.01; N, 8.98. Found: C, 65.7; H, 3.9; N, 8.9.

4.4.4. Compound 14e. Colorless prisms; mp 164–165°C (from AcOEt); ^{1}H NMR (500 MHz, $CDCl_3$) δ 1.23 (6H, t, *J*=7.1 Hz, Et-2), 3.96–4.00 (4H, m, Et-1), 4.13 (1H, s, CH), 7.07–7.14 (3H, m), 7.22–7.28 (1H, m), 7.46–7.53 (1H, m); ^{13}C NMR (125.7 MHz) δ 13.0, 37.6, 57.3, 133.6, 135.2, 137.1, 140.1, 141.3, 148.9, 150.8, 166.1, 185.2; IR ($CHCl_3$) ν 1679, 1576 cm^{-1}; MS (ESI) *m/z* 289 (M^++H). Anal. calcd for $C_{15}H_{16}N_2O_4$: C, 62.49; H, 5.59; N, 9.72. Found: C, 62.6; H, 5.6; N, 9.8.

4.4.5. Compound 14f. Colorless prisms; mp 212–213°C (from CH_2Cl_2/AcOEt); ^{1}H NMR (500 MHz, $CDCl_3$) δ 4.49 (1H, s, CH), 7.05–7.10 (3H, m), 7.14–7.21 (1H, m), 7.32 (4H, d, J=7.5 Hz, *o*-Ph), 7.40 (2H, t, J=7.3 Hz, *p*-Ph), 7.45 (4H, dd, J=7.5, 7.3 Hz, *m*-Ph), 7.52–7.59 (1H, m); ^{13}C NMR (125.7 MHz) δ 57.7, 128.5, 128.9, 133.7, 134.6, 135.5, 137.3, 140.3, 141.3, 148.8, 151.0, 166.3, 185.5; IR ($CHCl_3$) ν 1700, 1570 cm^{-1}; MS (ESI) *m/z* 385 (M^++H). Anal. calcd for $C_{23}H_{16}N_2O_4$: C, 71.87; H, 4.20; N, 7.29. Found: C, 71.7; H, 4.1; N, 7.3.

4.5. General synthetic procedure for 11a–c·BF_4^- and 1e,f·BF_4^- from 14a–c and 14e,f

A solution of **14a–c** and **14e,f** (0.5 mmol) in Ac_2O (2.5 mL) and 42% aq. HBF_4 (0.5 mL) was stirred at 0°C for 1 h. To the mixture was added Et_2O (50 mL) and the precipitates were collected by filtration to give **11a–c**·BF_4^- and **12a,c**·BF_4^- and **11e,f**·BF_4^-. The results are summarized in Table 2.

4.5.1. A mixture of 11a·BF_4^- and 12a·BF_4^-. Yellow powder; mp 243–246°C (from CH_3CN/Et_2O, decomp.); IR (KBr) ν 3382, 2790, 1718, 1685, 1265, 1084 cm^{-1}; MS (FAB) *m/z* 229 (M^+-BF_4; HRMS calcd for $C_{12}H_9N_2O_3BF_4$: 229.0613 ($M-BF_4$). Found: 229.0617 (M^+-BF_4). Anal. calcd for $C_{12}H_9N_2O_3BF_4$: C, 45.61; H, 2.87; N, 8.86. Found: C, 46.0; H, 2.9; N, 9.0.

4.5.2. Compound 11a·BF_4^-. ^{1}H NMR (500 MHz, CD_3CN) δ 3.67 (3H, s, Me), 8.67–8.75 (2H, m), 8.77–8.85 (1H, m), 9.04–9.09 (1H, m), 9.44 (1H, d, J=10.4 Hz, H-1), 9.89 (1H, br s, NH); ^{13}C NMR (150.9 MHz, CD_3CN) δ 30.7, 98.9, 135.3, 136.5, 138.8, 139.7, 144.7, 148.1, 148.6, 149.0, 157.3, 163.1.

4.5.3. Compound 11b·BF_4^-. Yellow prisms; mp 238–239°C (from CH_3CN/Et_2O, decomp.); ^{1}H NMR (500 MHz, CD_3CN) δ 1.00 (3H, t, J=7.4 Hz, Bu-4), 1.47 (2H, tq, J=7.8, 7.4 Hz, Bu-3), 1.84 (2H, quint, J=7.8 Hz, Bu-2), 4.21 (2H, t, J=7.8 Hz, Bu-1), 8.70–8.76 (2H, m), 8.80–8.84 (1H, m), 9.05–9.08 (1H, m), 9.43 (1H, d, J=9.1 Hz, H-1), 9.84 (1H, s, NH); ^{13}C NMR (150.9 MHz, CD_3CN) δ 13.9, 20.5, 30.7, 45.3, 99.1, 135.4, 139.7, 144.7, 148.2, 148.7, 149.1, 149.5, 157.5, 163.4, 167.6; IR (KBr) ν 3241, 2786, 1715, 1643, 1231, 1084 cm^{-1}; MS (FAB) *m/z* 271 (M^+-BF_4); HRMS calcd for $C_{15}H_{15}N_2O_3BF_4$: 271.1083 ($M-BF_4$). Found: 271.1065 (M^+-BF_4). Anal. calcd for $C_{15}H_{15}N_2O_3BF_4$: C, 50.31; H, 4.22; N, 7.8. Found: C, 50.1; H, 4.2; N, 7.8.

4.5.4. Compound 11c·BF_4^-. Orange prisms; mp 241–243°C (from CH_3CN/Et_2O, decomp.); ^{1}H NMR (500 MHz, CD_3CN) δ 7.59–7.62 (2H, m, *o*-Ph), 7.68–7.71 (3H, m, *m*, *p*-Ph), 8.69 (1H, dd, J=9.8, 9.6 Hz, H-4), 8.77 (1H, dd, J=10.2, 9.6 Hz, H-3), 8.86 (1H, dd, J=10.3, 10.2 Hz, H-2), 8.90 (1H, d, J=9.8 Hz, H-5), 9.53 (1H, d, J=10.3 Hz, H-1), 10.03 (1H, br s, NH); ^{13}C NMR (125.7 MHz, CD_3CN) δ 99.3, 129.0, 131.2, 132.0, 132.1, 135.8, 140.3, 145.0, 148.7, 148.8, 149.4, 157.5, 163.2, 166.9 (one carbon overlapping); IR (KBr) ν 3261, 1749, 1711, 1264, 1084 cm^{-1}; MS (FAB) *m/z* 291 (M^+-BF_4); HRMS calcd for $C_{17}H_{11}N_2O_3BF_4$: 291.0769 ($M-BF_4$). Found: 291.0784 (M^+-BF_4). Anal. cald for $C_{17}H_{11}N_2O_3BF_4$: C, 54.01; H, 2.93; N, 7.41. Found: C, 53.7; H, 2.8; N, 7.4.

4.5.5. Compound 11e·BF_4^-. Yellow prisms; mp 204–205°C (from CH_3CN/Et_2O); ^{1}H NMR (500 MHz, CD_3CN) δ 1.27 (3H, t, J=7.3 Hz, Et-2), 1.47 (3H, t, J=7.3 Hz, Et-2), 4.10 (2H, q, J=7.3 Hz, Et-1), 4.31 (2H, q, J=7.3 Hz, Et-1), 8.70–8.76 (2H, m, H-3, 4), 8.79–8.85 (1H, m, H-2), 9.05–9.09 (1H, m, H-5), 9.52 (1H, d, J=10.1 Hz, H-1); ^{13}C NMR (150.9 MHz, CD_3CN) δ 12.9, 13.4, 38.3, 41.5, 98.4, 135.1, 139.5, 144.5, 147.9, 148.5, 149.1, 149.7, 157.5, 163.0, 165.9; IR (KBr) ν 1724, 1675, 1272, 1085 cm^{-1}; MS (FAB) *m/z* 271 (M^+-BF_4); HRMS calcd for $C_{15}H_{15}N_2O_3BF_4$: 271.1083 ($M-BF_4$). Found: 271.1094 (M^+-BF_4). Anal. calcd for $C_{15}H_{15}N_2O_3BF_4$: C, 50.31; H, 4.22; N, 7.8. Found: C, 50.4; H, 4.0; N, 7.9.

4.5.6. Compound 11f·BF_4^-. Orange prisms; mp 289–291°C (from CH_3CN/Et_2O, decomp.); ^{1}H NMR (500 MHz, CD_3CN) δ 7.43–7.45 (4H, m, *o*-Ph), 7.56 (1H, t, J=7.3 Hz, *p*-Ph), 7.61 (1H, t, J=7.3 Hz, *p*-Ph), 7.67–7.69 (2H, m, *m*-Ph), 7.71–7.74 (2H, m, *m*-Ph), 8.73 (1H, dd, J=10.2, 9.9 Hz, H-4), 8.80 (1H, dd, J=10.2, 9.4 Hz, H-3), 8.88 (1H, dd, J=10.2, 9.4 Hz, H-2), 8.96 (1H, d, J=9.9 Hz, H-5), 9.58 (1H, d, J=10.2 Hz, H-1); ^{13}C NMR (150.9 MHz, CD_3CN) δ 98.8, 128.9, 129.5, 130.4, 130.6, 131.2, 132.1, 132.4, 135.5, 135.8, 140.3, 145.0, 148.7, 148.9, 148.9, 150.3, 157.8, 163.1, 165.6; IR (KBr) ν 1705, 1640, 1265, 1084 cm^{-1}; MS (FAB) *m/z* 367 (M^+-BF_4); HRMS calcd for $C_{23}H_{15}N_2O_3BF_4$: 367.1083 ($M-BF_4$). Found: 367.1076 (M^+-BF_4). Anal. calcd for $C_{23}H_{15}N_2O_3BF_4$: C, 60.82; H, 3.33; N, 6.17. Found: C, 60.8; H, 3.2; N, 6.2.

4.6. Protonation of 5a–c to give 12a–c·BF_4^-

A solution of **5a–c** (0.3 mmol) in Ac_2O (2 cm^3) and 42% aq. HBF_4 (0.4 cm^3) was stirred at 0°C for 1 h. To the reaction mixture was added Et_2O (30 cm^3) and the precipitates were collected by filtration to give **12a–c**·BF_4^-. The results are summarized in Table 2.

4.6.1. Compound 12a·BF_4^-. Yellow powder; mp 255–258°C (from CH_3CN/Et_2O, decomp.); ^{1}H NMR (500 MHz, CD_3CN) δ 3.37 (3H, s, Me), 8.67–8.75 (2H, m), 8.77–8.85 (1H, m), 9.01–9.04 (1H, m), 9.50 (1H, d, J=9.6 Hz, H-1), 9.89 (1H, br s, NH); ^{13}C NMR (150.9 MHz, CD_3CN) δ 28.2, 98.1, 134.8, 139.3, 144.5, 147.7, 148.4, 148.9, 150.3, 158.5, 163.3, 166.6; IR (KBr) ν 3447, 2535, 1723, 1685, 1254, 1084 cm^{-1}; MS (FAB) *m/z* 229 (M^+-BF_4); HRMS calcd for $C_{12}H_9N_2O_3BF_4$: 229.0613 ($M-BF_4$). Found: 229.0613 (M^+-BF_4). Anal. calcd for $C_{12}H_9N_2O_3BF_4$+1/4HBF_4: C, 42.65; H, 2.76; N, 8.29. Found: C, 42.5; H, 2.5; N, 8.3.

4.6.2. Compound 12b·BF_4^-. Yellow powder; mp 205–206°C (from CH_3CN/Et_2O); ^{1}H NMR (500 MHz, CD_3CN) δ 0.96 (3H, t, J=7.4 Hz, Bu-4), 1.40 (2H, quint., J=7.4 Hz, Bu-3), 1.65 (2H, quint, J=7.4 Hz, Bu-2), 4.00 (2H, t, J=7.4 Hz, Bu-1), 5.20 (1H, br s, NH), 8.71–8.79 (2H, m), 8.82–8.87 (1H, m), 9.05–9.10 (1H, m), 9.52 (1H, d, J=9.1 Hz, H-1); ^{13}C NMR (125.7 MHz, CD_3CN) δ 14.1, 20.8, 30.5, 42.1, 98.4, 135.3, 139.7, 144.9, 148.2, 148.7, 149.1, 149.8, 158.5, 163.4, 166.2; IR (KBr) ν 3397, 2513,

1734, 1678, 1261, 1084 cm^{-1}; MS (FAB) *m/z* 271 (M^+-BF_4); HRMS calcd for $C_{15}H_{15}N_2O_3BF_4$: 271.1083 ($M-BF_4$). Found: 271.1085 (M^+-BF_4). Anal. calcd for $C_{15}H_{15}N_2O_3BF_4+1/2HBF_4$: C, 44.82; H, 3.89; N, 6.97. Found: C, 45.0; H, 3.6; N, 6.9.

4.6.3. Compound 12c·BF_4^-. Yellow powder; mp 203–204°C (from CH_3CN/Et_2O); ^1H NMR (500 MHz, CD_3CN) δ 4.28 (1H, br s, NH), 7.34–7.36 (2H, m, *o*-Ph), 7.49–7.60 (3H, m, *m*, *p*-Ph), 8.71–8.79 (2H, m), 8.79–8.84 (1H, m), 9.06–9.12 (1H, m), 9.45 (1H, d, J=11.2 Hz, H-1); ^{13}C NMR (125.7 MHz, CD_3CN) δ 98.8, 129.8, 130.4, 130.6, 135.4, 139.7, 145.0, 148.3, 148.8, 149.1, 150.1, 158.6, 163.5, 166.7; IR (KBr) ν 3421, 2539, 1748, 1707, 1263, 1084 cm^{-1}; MS (FAB) *m/z* 291 (M^+-BF_4); HRMS cacld for $C_{17}H_{11}N_2O_3BF_4$: 291.0769 ($M-BF_4$). Found: 291.0776 (M^+-BF_4). Anal. calcd for $C_{17}H_{11}N_2O_3BF_4+1/3HBF_4$: C, 50.12; H, 2.80; N, 6.88. Found: C, 50.6; H, 3.0, N, 7.0.

4.7. Alkaline hydrolysis of mixtures of 11a–c·BF_4^- and 12a–c·BF_4^-

To a stirred solution of mixtures **11a–c**·BF_4^- and **12a–c**·BF_4^- (0.3 mmol) in EtOH (6 cm^3) was added saturated aq. K_2CO_3 (3 cm^3) and the mixture was stirred at 80°C for 12 h. After evaporation of the solvent, the residue was dissolved in 3% HCl and the mixture was stirred for 1 h. The mixture was extracted with CH_2Cl_2 and the extract was dried over Na_2SO_4. The residue was concentrated in vacuo to give **14a–c**, which were identified on the basis of the comparison of the physical data with those reported in the literature.[15]

4.8. Cyclic voltammetry of 8a–f, 11a–f·BF_4^- and 12a–c·BF_4^-

The redox potentials of **8a–f**, **11a–f**·BF_4^- and **12a–c**·BF_4^- were determined by means of CV-27 voltammetry controller (BAS Co). A three-electrode cell was used, consisting of Pt working and counter electrodes and a reference $Ag/AgNO_3$ electrode. Nitrogen was bubbled through an acetonitrile solution (4 mL) of each compound (0.5 mmol dm^{-3}) and Bu_4NClO_4 (0.1 mol dm^{-3}) to deaerate it. The measurements were made at a scan rate of 0.1 V s^{-1} and the voltammograms were recorded on a WX-1000-UM-019 (Graphtec Co) X-Y recorder. Immediately after the measurements, ferrocene (0.1 mmol) ($E_{1/2}$=+0.083) was added as the internal standard, and the observed peak potentials were corrected with reference to this standard. The compounds exhibited no reversible redox wave: each of the redox potentials was measured through independent scan, and they are summarized in Tables 1 and 4.

4.9. X-Ray structure determination of 11c·BF_4^-[†]

Orange prisms, $C_{17}H_{11}N_2O_3$, M=378.1, monoclinic, space group $P2_1/n$, a=7.3640(2), b=12.5380(3), c=17.0902(6) Å, β=97.190(1)°, V=1565.53(8) $Å^3$, Z=4, Dc=1.604 g cm^{-3}, crystal dimensions 0.40×0.20×0.20 mm^3. Data were measured in a Rigaku RAXIS-RAPID radiation diffractometer with graphite monochromated Mo K_α radiation. A total 13069 reflections were collected, using the $\omega-2\theta$ scan technique to a maximum 2θ value of 55.0°. The structure was solved by direct methods and refined by a full-matrix least-squares method using SIR92 structure analysis software,[27] with 256 variables and 2019 observed reflections [$I>3.00\sigma(I)$]. The non-hydrogen atoms were refined anisotropically. The weighing scheme $w=[\sigma_c^2(F_0)+0.0020\times F_0^2]^{-1}$ gave satisfactory agreement analysis. The final R and R_w values were 0.041 and 0.057. The maximum peak and minimum peak in the final difference map were 0.31 and $-0.26e^-/Å^3$.

[†] CCDC reference number 202050.

Acknowledgements

Financial support from a Waseda University Grant for Special Research Project and 21COE 'Practical Nanochemistry' from MEXT, Japan is gratefully acknowledged. We thank the Materials Characterization Central Laboratory, Waseda University for technical assistance with the spectral data, elemental analyses and X-ray analysis.

References

1. Ogliaruso, M. A.; Romanelli, M. G.; Becker, E. I. *Chem. Rev.* **1965**, *65*, 261–367.
2. Bertelli, D. J.; Andrews, T. G., Jr.; Crew, P. O. *J. Am. Chem. Soc.* **1969**, *91*, 5286–5296.
3. Hollenstein, R.; Mooser, A.; Neuenschwander, M.; von Philipsborn, W. *Angew. Chem.* **1974**, *87*, 595–596.
4. Oda, M.; Funamizu, M.; Kitahara, Y. *Bull. Chem. Soc. Jpn* **1969**, *42*, 2386–2387.
5. (a) Shimanouchi, H.; Ashida, T.; Sasada, Y.; Kakudo, M.; Murata, I.; Kitahara, Y. *Bull. Chem. Soc. Jpn* **1965**, *38*, 1230. (b) Mori, A.; Yin, B. Z.; Endo, A.; Takeshita, H. *Chem. Lett.* **1992**, 855–858.
6. Shimanouchi, H.; Sasada, Y.; Kabuto, C.; Kitahara, Y. *Tetrahedron Lett.* **1968**, *9*, 5053–5054.
7. (a) Ikeda, Y.; Yin, B. Z.; Kato, N.; Mori, A.; Takeshita, H. *Bull. Chem. Soc. Jpn* **1996**, *69*, 1319–1327. (b) Ikeda, Y.; Yin, B. Z.; Kato, N.; Mori, A.; Takeshita, H. *Chem. Lett.* **1992**, 1453–1456. (c) Ikeda, Y.; Yin, B. Z.; Kato, N.; Mori, A.; Takeshita, H. *Heterocycles* **1993**, *36*, 1725–1728.
8. Takahashi, K. *J. Synth. Org. Chem. Jpn* **1986**, 806–818, (*Chem. Abstr.* **1987**, *107*, 115439v); and references cited therein.
9. Waele, V. D.; Schmidhammer, U.; Mrozek, T.; Daub, J. *J. Am. Chem. Soc.* **2002**, *124*, 2438–2439.
10. Walsh, C. *Acc. Chem. Res.* **1986**, *19*, 216–221, and references cited therein.
11. Yoneda, F.; Tanaka, K. *Med. Res. Rev.* **1987**, *4*, 477–506, and references cited therein.
12. Yoneda, F.; Kokel, B. *Chemistry and Biochemistry of Flavoenzymes*; Muller, F., Ed.; CRC Press: Boca Raton, 1991; Vol. 1, pp 121–169 and references cited therein.
13. Yoneda, F.; Hirayama, R.; Yamashita, M. *Chem. Lett.* **1980**, 1157–1160.
14. Nitta, M.; Tajima, Y. *Synthesis* **2000**, 651–654.
15. Takayasu, T.; Mizuta, Y.; Nitta, M. *Heterocycles* **2001**, *54*, 601–606.

16. Naya, S.; Nitta, M. *J. Chem. Soc., Perkin Trans. 1* **2000**, 2777–2781.
17. Naya, S.; Nitta, M. *J. Chem. Soc., Perkin Trans. 1* **2000**, 2427–2735.
18. Naya, S.; Nitta, M. *J. Chem. Soc., Perkin Trans. 2* **2001**, 275–281.
19. Naya, S.; Isobe, M.; Hano, Y.; Nitta, M. *J. Chem. Soc., Perkin Trans. 2* **2001**, 2253–2262.
20. Naya, S.; Sakakibara, T.; Nitta, M. *J. Chem. Soc., Perkin Trans. 2* **2001**, 1032–1037.
21. Naya, S.; Miyama, H.; Yasu, K.; Takayasu, T.; Nitta, M. *Tetrahedron* **2003**, *59*, 1811–1821.
22. Seitz, G.; Olsen, R. A. *Angew. Chem.* **1976**, *88*, 142–143.
23. Nozoe, T.; Mulai, T.; Osaka, K.; Shishido, N. *Bull. Chem. Soc. Jpn* **1961**, *34*, 1384–1390.
24. Frisch, M. J.; Trucks, G. W.; Schlegel, H. B.; Scuseria, G. E.; Robb, M. A.; Cheeseman, J. R.; Zakrzewski, V. G.; Montgomery, J. A., Jr.; Stratmann, R. E.; Burant, J. C.; Dapprich, S.; Millam, J. M.; Daniels, A. D.; Kudin, K. N.; Strain, M. C.; Farkas, O.; Tomasi, J.; Barone, V.; Cossi, M.; Cammi, R.; Mennucci, B.; Pomelli, C.; Adamo, C.; Clifford, S.; Ochterski, J.; Petersson, G. A.; Ayala, P. Y.; Cui, Q.; Morokuma, K.; Salvador, P.; Dannenberg, J. J.; Malick, D. K.; Rabuck, A. D.; Raghavachari, K.; Foresman, J. B.; Cioslowski, J.; Ortiz, J. V.; Baboul, A. G.; Stefanov, B. B.; Liu, G.; Liashenko, A.; Piskorz, P.; Komaromi, I.; Gomperts, R.; Martin, R. L.; Fox, D. J.; Keith, T.; Al-Laham, M. A.; Peng, C. Y.; Nanayakkara, A.; Challacombe, M.; Gill, P. M. W.; Johnson, B.; Chen, W.; Wong, M. W.; Andres, J. L.; Gonzalez, C.; Head-Gordon, M.; Replogle, E. S.; Pople, J. A. Gaussian 98, Revision A.11; Gaussian, Inc.: Pittsburgh PA, 2001.
25. (a) Doering, W.; von, E.; Knox, L. H. *J. Am. Chem. Soc.* **1957**, *79*, 352–356. (b) Okamoto, K.; Komatsu, K.; Kinoshita, T.; Shingu, H. *Bull. Chem. Soc. Jpn* **1970**, *43*, 1901–1902.
26. (a) Biggs, A. I. *J. Chem. Soc.* **1956**, 2485–2488. (b) Brückmann, G.; Isaacs, S. D. *J. Am. Chem. Soc.* **1949**, *71*, 390–392. (c) Ridi, M.; Aldo, G. *Gazz. Chim. Ital.* **1952**, *82*, 13–22.
27. Altomare, A.; Burla, M. C.; Camalli, M.; Cascarano, M.; Giacovazzo, C.; Guagliardi, A.; Polidori, G. *J. Appl. Crystallogr.* **1994**, *27*, 435.